Journal of Applied Polymer Science

Composite Porous Membrane for Protecting High-Performance Fibers from Ultraviolet–Visible Radiation

Ahmed H. Hassanin,[1] Magdi A. Said,[2] Abdel-Fattah M. Seyam[1]
[1]College of Textiles, North Carolina State University, Raleigh, North Carolina 27695
[2]NASA Wallops Flight Facility, Wallops Island, Virginia 23337
Correspondence to: A.-F. M. Seyam (E-mail: aseyam@ncsu.edu)

ABSTRACT: High-strength fibers are used to produce high-strength-to-weight-ratio materials for applications such as composites, soft and hard body armor, bulletproof vests, and tendons for scientific balloons. Unfortunately, these fibers degrade when they are exposed to ultraviolet–visible (UV–vis) radiation. The objective of this research was to develop systems to improve the UV resistance of such fibers. Composite porous membranes from a polyurethane (PU) matrix loaded with rutile titanium dioxide (TiO_2) nanoparticles were developed to protect a braid made of polybenzobisoxazole (PBO) yarns. The PU membranes loaded with TiO_2 nanoparticles were prepared by a phase-inversion technique. The effects of the amount of TiO_2 nanoparticles on the composite membrane morphological structure and UV–vis light transmission were evaluated. The results show that when the concentration of TiO_2 nanoparticles was increased, the porosity of the membrane and its UV–vis blocking effectiveness increased. The UV–vis protection was evaluated by the wrapping of the PBO braid with the composite membranes and exposed to UV–vis radiation. The strength loss of the PBO fiber due to exposure was decreased from 75% for the unprotected sample to 7.8% for the protected sample in the PU loaded with 4% TiO_2 nanoparticles. © 2012 Wiley Periodicals, Inc. J. Appl. Polym. Sci. 128: 1297–1303, 2013

KEYWORDS: composites; degradation; membranes; nanoparticles; nanowires and nanocrystals; radiation

Received 29 June 2011; accepted 13 August 2012; published online 17 October 2012
DOI: 10.1002/app.38476

INTRODUCTION

High-strength fibers, such as polybenzobisoxazole (PBO), Kevlar, and Vectran, are used to produce composites, bulletproof vests, tendons of giant scientific balloons, and other high-performance products. Unfortunately, these fibers are known to degrade upon exposure to UV radiation, and this causes premature failure. Many attempts have been made to improve the UV resistance of high-performance fibers with little success.[1–9] Although these attempts shed light on good approaches for protecting high-performance fibers, they suffered drawbacks. The protective layer uniformity, weight added, durability, and UV absorber particles' distribution in the protective layer have not been fully addressed. Additionally, work on single fibers[5,6,8] requires significant weight add-on of the protective layer to cover the high surface area of individual fibers, and this leads to a reduction in the high strength-to-weight ratio of these fibers. Although prior studies on the development of the UV protective layer have achieved significant improvements in the protection level, their deficiency in keeping a high strength-to-weight ratio and durability of the protective layer need to be addressed. Therefore, research is still needed to develop new materials that have the ability to protect the high-performance fibers with minimum weight added and achieve maximum protection from UV–vis radiation. Because it is very difficult to use approaches that are being used to protect traditional polymers, such as polyester and nylon, from UV,[10,11] the main goal of this study was to protect high-performance fibers from UV degradation with a composite porous membrane from a polyurethane (PU) matrix loaded with nanoscale UV absorbers. Our approach dealt with the use of the protective membrane to cover the entire product from high-performance fibers rather than a single fiber. For this research, the selected product was a braid from PBO, which is also known as *Zylon*. The protective composite membrane was extremely lightweight so that it could maintain the high strength-to-weight ratio of the hybrid structure, as shown in Figure 1.

EXPERIMENTAL

Materials

The PBO braid was manufactured from 1500 denier yarn by Cortland Cable Co. (Cortland, NY). In total, 32 yarns were used to form the braid. Thus, the total braid denier was approximately 48,000 (32 × 1500). The braid interlacing structure was 2 × 2. Rutile titanium dioxide (TiO_2) nanoparticles were used

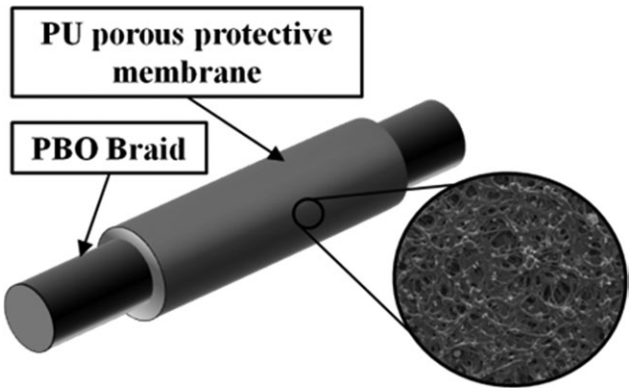

Figure 1. Schematic presentation for the PBO braid sheathed with a PU porous protective membrane from UV–vis light radiation.

as a UV–vis light blocker. The shape of these particles was cylindrical, and they were 10 nm in diameter and 40 nm in length. The material density was 4.23 g/cm^3. A standard aliphatic PU was used as the polymeric matrix, and it was loaded with the TiO_2 nanoparticles. The organic solvent used to prepare the membranes was *N,N*-dimethylacetamide (DMAc; 99% pure).

Composite Membrane Formation and Experimental Design

PU was dissolved in 99% pure DMAc. The solution was kept under stirring at room temperature overnight for 12 h to achieve complete dissolution. The TiO_2 nanoparticles were first dispersed in DMAC to break the agglomeration by vigorous stirring for 30 min, and then, the mix was added to a PU solution. The final concentration of PU in DMAC was 10 wt %. The PU solution with TiO_2 nanoparticles was kept under vigorous stirring overnight with a mechanical stirrer for 12 h to ensure good dispersion of the nanoparticles in the PU solution. The TiO_2 nanoparticle contents were 1, 2, and 4% on the basis of the PU weight. The PU solution with nanoparticles was spread onto a glass plate with a uniform thickness with a micrometer-adjustable film applicator. The cast membrane was kept on the glass plate for 30 min and was then immersed in a water bath and left in the bath overnight for 12 h. The membrane was removed and hung under a ventilation hood until it was completely dry.

Additional samples were produced by the evaporation method to illustrate the differences in the morphology between the two methods (the coagulation and evaporation techniques). The sample prepared by evaporation did not contain TiO_2. In the evaporation method, the PU solution was spread onto a glass plate with a uniform thickness with the micrometer-adjustable film applicator. The cast membrane was kept under a ventilation hood for 24 h, was then washed with running water, and was then dried for another 24 h.

Table I shows the experimental design that was implemented to optimize the parameters to reveal the lowest percentage of rutile TiO_2 nanoparticles and the membrane thickness (weight) with the highest UV–vis light protection.

Membrane Characterization

Membrane Morphology. A JEOL 6400F field emission electron microscope (Joel Inc., Peabody, MA) was used to investigate the morphology of the PU membranes. The data were gathered at an acceleration voltage of 5 kV and at different magnifications.

UV and Visible Light Transmittance. Ultraviolet–visible (UV–vis) spectroscopy analysis was performed with a Cary 3 UV–vis spectrophotometer (Agilent Technologies, Santa Clara, CA) to determine the UV–vis light transmittance for the PU membranes. Specimens that were 20 × 20 mm^2 were prepared. Each specimen was mounted in an integrating sphere (DRA-CA-301), which was a special attachment for measuring the transmittance and reflection for membranes and fabrics.

Weathering. The PBO braids were wrapped with the PU membrane, and then, the samples were exposed to UV–vis radiation in aCi3000 Atlas weatherometer (Atlas, Chicago, IL), which had a xenon lamp jacketed in quartz inner and outer filters. With this setup, the lamp emitted radiation within a range of wavelengths (230–750 nm) that simulated extraterrestrial solar radiation (altitude ≈ 40,000 m).

Mechanical Properties. Tensile testing for individual yarns that were unraveled from the braid before and after exposure were performed according to ASTM D 2256 with a Renew MTS machine (MTS, Eden Prairie, MN). The gauge length and crosshead speed were 25 and 30 cm/min, respectively. The grip pressure was between 0.5 and 0.7 MPa (80–100 psi).

RESULTS AND DISCUSSION

Morphological Structure of the PU Membranes

Field emission scanning electron microscopy (FE-SEM) images of the blank PU membrane (0% TiO_2) prepared by different methods (coagulation and evaporation) are presented in Figures 2 (evaporated) and 3 (coagulated). As shown in the scanning electron microscopy (SEM) images, the membrane produced by the evaporation method was denser and did not exhibit voids or pores, whereas the membrane produced by the coagulation method exhibited voids and pores. The morphological structure of the coagulated membrane was spongelike in structure. This significant difference in the morphological structure between the two membranes was due to the so-called phase inversion process in the coagulated membrane. In this process, the polymer solution was immersed into a coagulation bath, which was water in this case. The polymer solution underwent two stages, as illustrated in the ternary phase diagram (Figure 4). The first was liquid–liquid phase separation; in this stage, the completely miscible solution entered a two-phase region (from region I to region II, the solvent and nonsolvent regions, respectively). The second was the solidification stage, in which the polymer went from region II to region III. It was suggested in refs. 12 and 13 that if a cast polymer solution enters the solidification region

Table I. Experimental Design of the PU Membranes Loaded with Rutile TiO_2 Nanoparticles

Variable	Level
TiO_2 in PU (%)	4 (0, 1, 2, 4)
Membrane areal density (g/m^2)	4
Total number of treatments	4 × 4 = 16

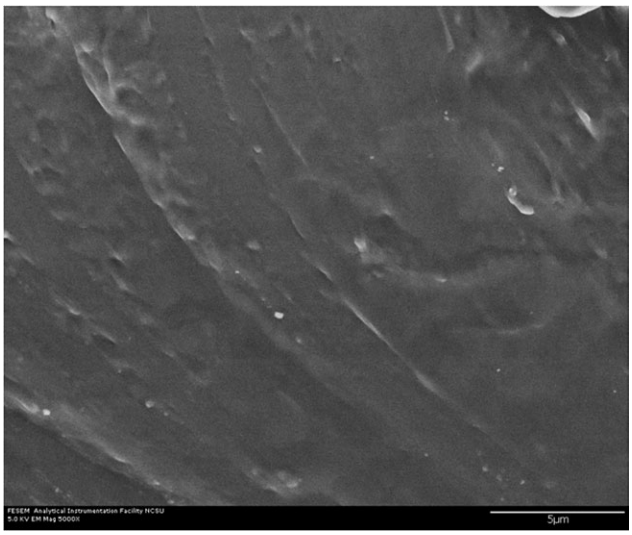

Figure 2. FE-SEM cross-sectional image of the blank PU membrane prepared by the evaporation technique.

directly, from region I to region III, the resulting membrane will be dense in structure, and this was the situation with the evaporation method. If the cast polymer solution entered the liquid–liquid phase separation, the solidification region, from region I to region II and then to region III, the resulting membrane was porous in structure.

Figures 5–9 show the morphological structures of membranes that were produced by the coagulation method and different concentrations of TiO_2 nanoparticles (1, 2, and 4%). As shown in these images, when the concentration of TiO_2 was increased in the polymer solution, the voids increased, and the structure became more porous and spongelike. This observation was confirmed by the values of the membrane density (Table II and Figure 10). By increasing the concentration of TiO_2, the membrane volume density (determined from the thickness and areal

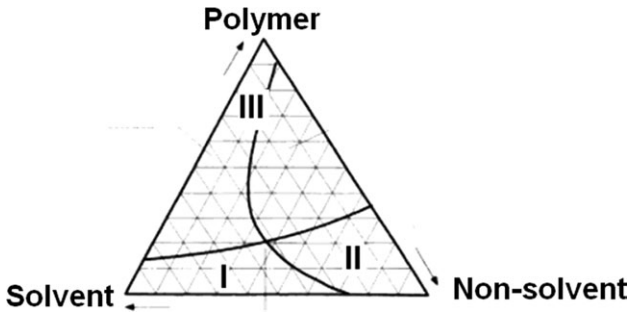

Figure 4. Ternary phase diagram for the membrane formed by phase inversion.[14]

density measurements of five observations each) decreased, and this proved that the voids and pores increased with increasing nanoparticle percentage. The results of Table II and Figure 10 also indicate the values of the volume density of the coagulated membranes were much lower than those of the membrane prepared by the evaporation technique.

In the work of Soroko and Livingston,[15] the effect of TiO_2 nanoparticles on the morphology of polyimide membranes was investigated. The results show that the microvoids were decreased with increasing TiO_2 concentration. The author attributed this observation to the effect of TiO_2, which increased \the viscosity of the solution; this may have acted as a void suppressant. In addition, TiO_2 particles acted as a nucleating agent, which may have led to a decrease in the void formation. In another work by Li et al.,[16] the effect of TiO_2 nanoparticles on the surface morphology of poly(ether sulfone) (PES) was studied. PES membranes were prepared by the combination of two processes, namely, vapor-induced phase separation and the immersion precipitation technique. The PES membranes were loaded with different concentrations of TiO_2. The results show that in case of 1–2% TiO_2, a highly porous structure was

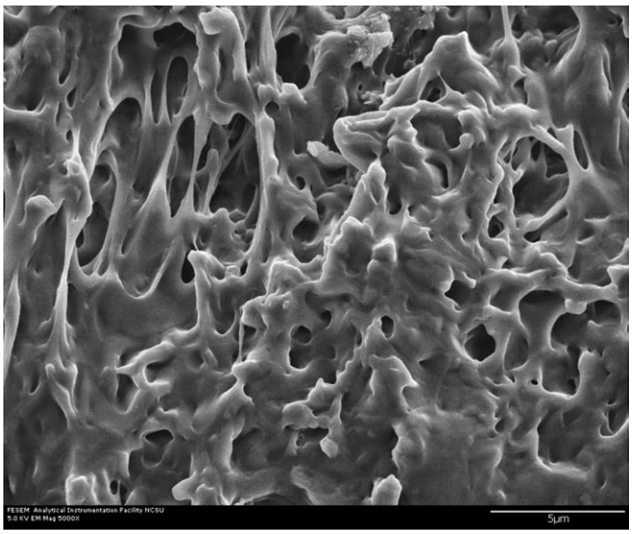

Figure 3. FE-SEM cross-sectional image of the blank PU membrane prepared by the coagulation method.

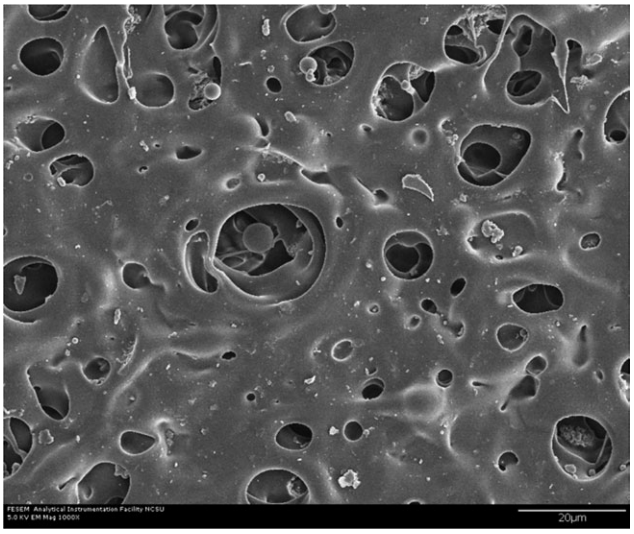

Figure 5. FE-SEM top-view image of the PU membrane containing 1% TiO_2.

Applied Polymer SCIENCE

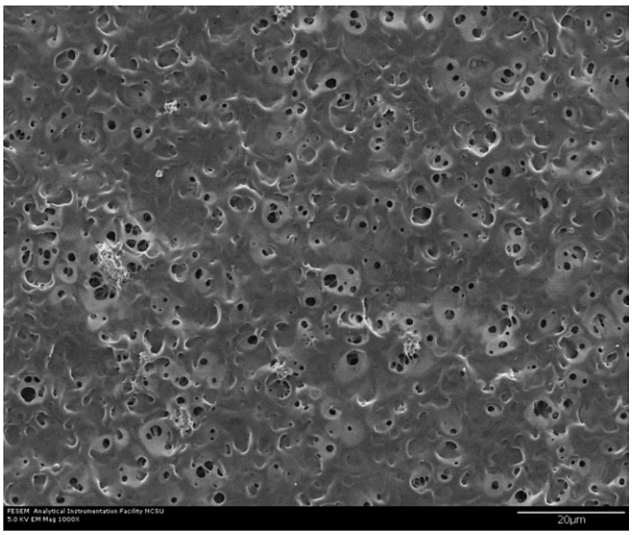

Figure 6. FE-SEM top-view image of the PU membrane containing 2% TiO_2.

formed, especially at the top surface of membrane. When the amount of TiO_2 was increased over 2%, the structure became less porous, and an aggregation of TiO_2 nanoparticles started to be seen on the surface. The author attributed these observations to the effect of TiO_2 in viscosity and nucleation. In addition, the author attributed the effect of the low percentage of TiO_2 (1 and 2%) to the increase in the porosity of the membrane to the high surface area and hydrophilicity, which affected the mass transfer during the vapor-induced phase separation stage and helped in the penetration of humidity in air during this stage. Razmjou et al.[17] also investigated the effect of TiO_2 nanoparticles on the surface morphology of PES. The same observation was observed in that when the TiO_2 nanoparticles were introduced, the porosity increased, especially in the top surface layer. The same finding was confirmed in the work of Cao et al.,[18] where the effect of TiO_2 on the morphology of poly(vinylidene fluoride) was studied.

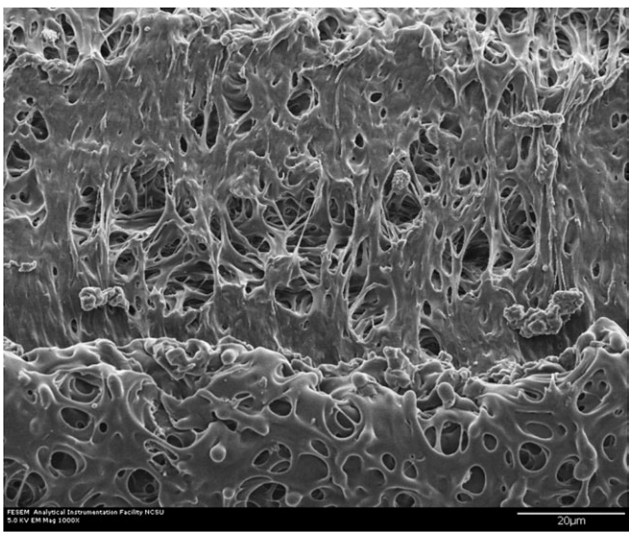

Figure 7. FE-SEM cross-sectional image of the PU membrane containing 2% TiO_2.

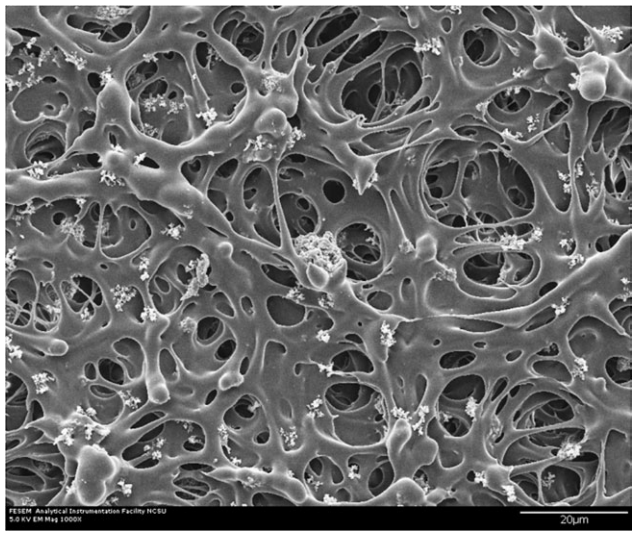

Figure 8. FE-SEM top-view image of the PU membrane containing 4% TiO_2.

Our results indicate that the increase in TiO_2 caused a reduction in the density of the composite structure, and this was supported by most of the previous work in this area. The explanation of the results is still unconfirmed and warrants additional research.

UV–Vis Transmittance and Reflection of the PU Membranes

Figure 11 shows the UV–vis transmittance for the two blank PU membranes prepared by coagulation and evaporation. The results show about a 45% reduction in the transmittance in the visible region and a more than 50% reduction in the UV region (300 to 400 nm) between the membrane that was produced by the evaporation method and the membrane that was produced by the coagulation method. This means that the coagulated membrane was more opaque; this could be seen through observation of the two membranes. This opaqueness was due to the

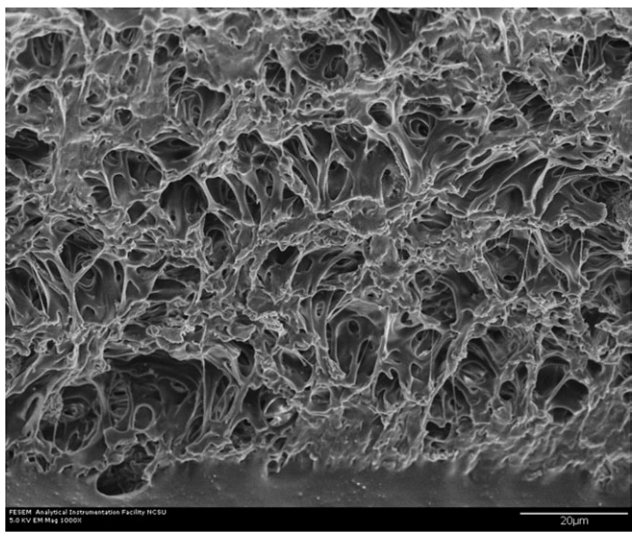

Figure 9. FE-SEM cross-sectional image of the PU membrane containing 4% TiO_2.

Table II. Density Values of the PU Membranes Loaded with Different Concentrations of TiO_2 Nanoparticles

	0% TiO_2 (evaporation)	0% TiO_2 (coagulation)	1% TiO_2 (coagulation)	2% TiO_2 (coagulation)	4% TiO_2 (coagulation)
Thickness of one layer (mm)	0.06	0.08	0.08	0.12	0.18
Areal density (g/m^2)	69.5	84.01	83.74	74.65	99.4
Volume density (g/cm^3)	1.158	1.050	1.047	0.622	0.552

irregular and porous morphological structure (Figure 3), which resulted in more light scattering compared to light transmission (Figures 11 and 12). In addition, there was a clear trend, shown by the results of Figure 13, in which the light transmittance decreased in both the UV and visible light regions when the number of membrane layers was increased.

Figures 14–16 show the UV–vis transmittance for the PU membranes loaded with 1, 2, and 4% TiO_2 nanoparticles, respectively. It was obvious that with increasing amount of TiO_2 and thickness of the membranes (increasing numbers of layers), the UV and visible light transmittance decreased; this was a good indication for better protection from such radiation. As shown in Figure 16, four layers of the composite membrane loaded with 4% TiO_2 blocked all the light in the UV and in the visible range.

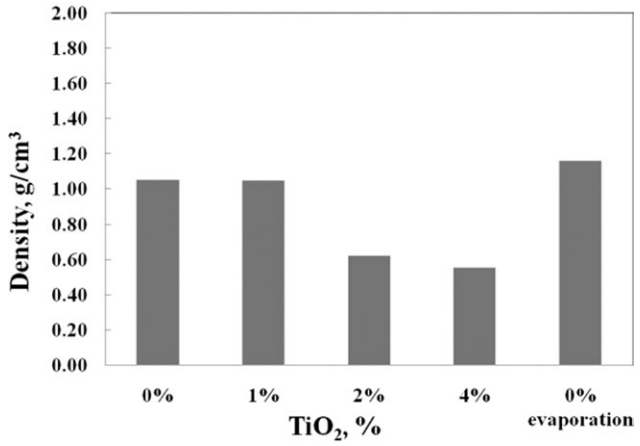

Figure 10. Density of the coagulated PU membrane loaded with different concentrations of TiO_2 nanoparticles as compared to the membrane prepared by the evaporation method.

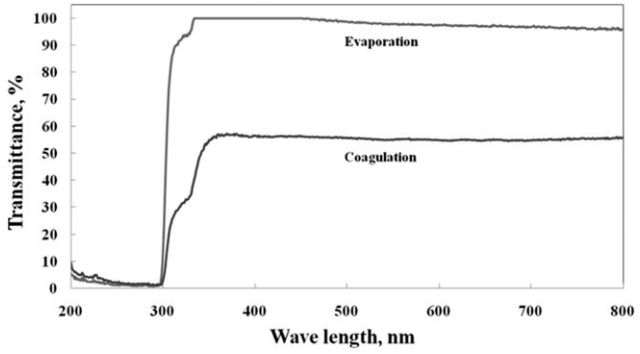

Figure 11. UV–vis light transmittances of the blank PU membranes.

Effect of the UV–Vis Exposure on the Tensile Strength of the PBO Yarns

According to the UV–vis transmittance, the best candidates of the composite membranes were chosen to protect the PBO braid from UV–vis exposure. Membranes loaded with 2 and 4% TiO_2 with one, two, and three layers were chosen. These six samples were wrapped around braids, and the wrapped samples were exposed to UV–vis in an Atlas weatherometer for 6 days.

Figure 17 shows the effect of weathering on the tensile strength of the PBO yarns unraveled from the PBO braid and covered by PU layers (one, two, and three layers) loaded with 2% TiO_2. There was a clear trend in which with increasing number of PU layers, an improvement in the tensile strength (or lower degradation) of the exposed braid was achieved. The same trend was observed in Figure 18, which shows the effect of weathering on the tensile strength of the PBO yarns unraveled from the PBO braid covered by PU layers (one, two, and three layers) loaded with 4% TiO_2. In Table III and Figure 19, we observed that the

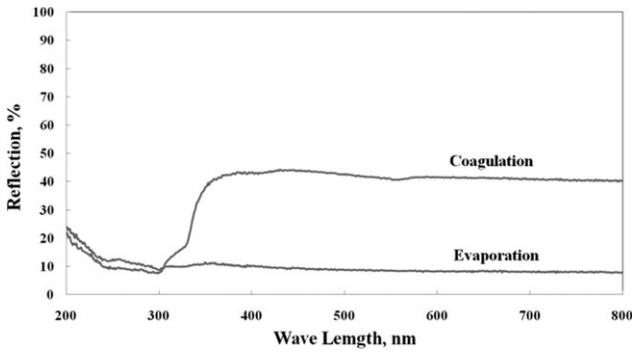

Figure 12. UV–vis light reflection of the blank PU membrane.

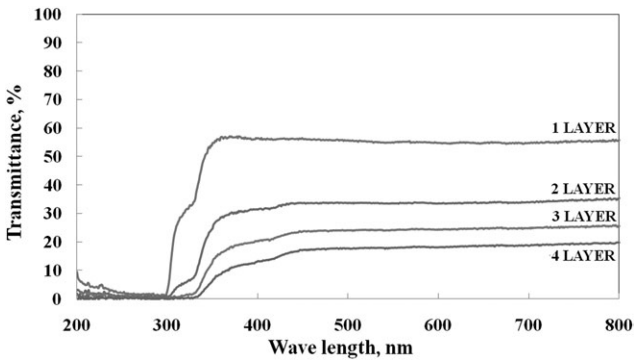

Figure 13. UV–vis light transmittances of the blank PU membrane in terms of the number of membrane layers.

Applied Polymer SCIENCE

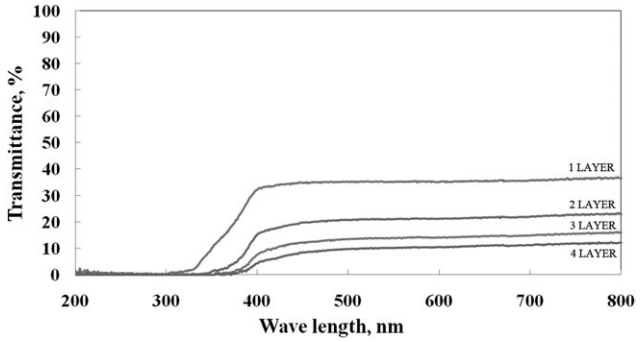

Figure 14. UV–vis light transmittances of the PU membrane containing 1% TiO_2.

maximum protection was achieved by three layers of PU loaded with 4% TiO_2. In this case, the loss in the tensile strength after 6 days of exposure was 7.84%; this was supported by the UV–vis transmittance curve, which indicated a high percentage of UV–vis blocking with a complete blockading of 100% in the UV region.

CONCLUSIONS

A range of composite porous membranes from a PU matrix loaded with TiO_2 nanoparticles was developed to protect PBO braids from UV–vis radiation. PU membranes loaded with TiO_2 in the range of 0–4% were prepared by phase-inversion coagulation and evaporation techniques, and their morphological structures were evaluated. The SEM images showed that the membranes produced by the evaporation method were denser and did not contain voids or pores, whereas the membranes produced by the coagulation method exhibited voids and pores.

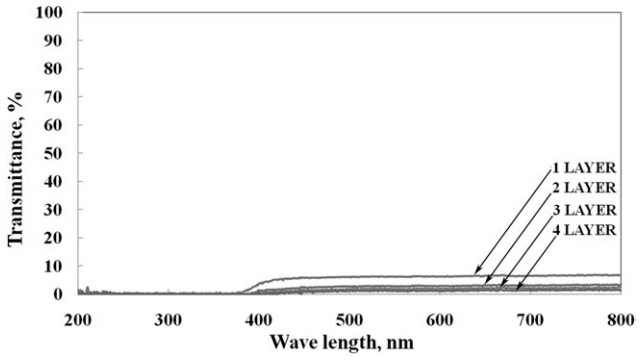

Figure 15. UV–vis light transmittances of the PU membrane loaded with 2% TiO_2.

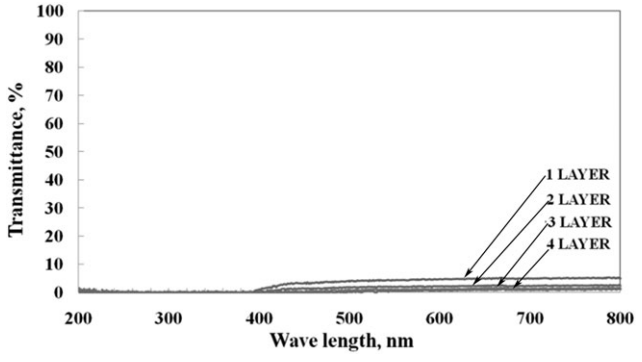

Figure 16. UV–vis light transmittances of the PU membrane containing 4% TiO_2.

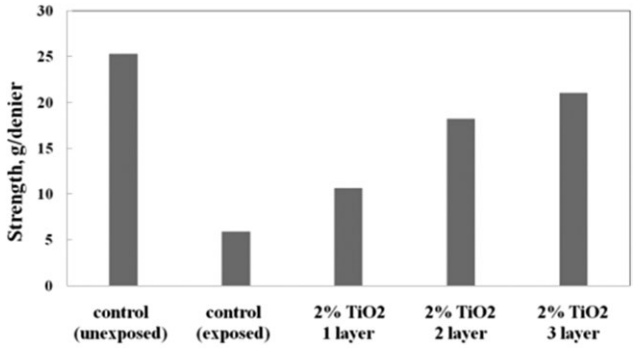

Figure 17. Tensile strength of the PBO yarns sheathed with PU layers containing 2% TiO_2 after 6 days of exposure.

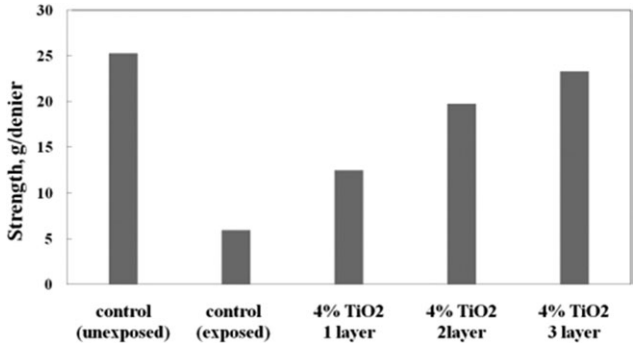

Figure 18. Tensile strength of the PBO yarns sheathed with PU layers containing 4% TiO_2 after 6 days of exposure UV–vis.

Table III. Tensile Strength of the PBO Yarn before and after 6 Days of Exposure to UV–Vis Radiatio

	Tensile strength (g/denier)		Tensile strength loss after exposure (%)
	Before exposure	After exposure	
Control sample (unsheathed)		5.90	76.68
PU 2% TiO_2			
One layer		10.62	57.99
Two layers		18.20	28.02
Three layers	25.29	21.00	16.95
PU 4% TiO_2			
One layer		12.45	50.79
Two layers		19.75	21.92
Three layers		23.31	7.84

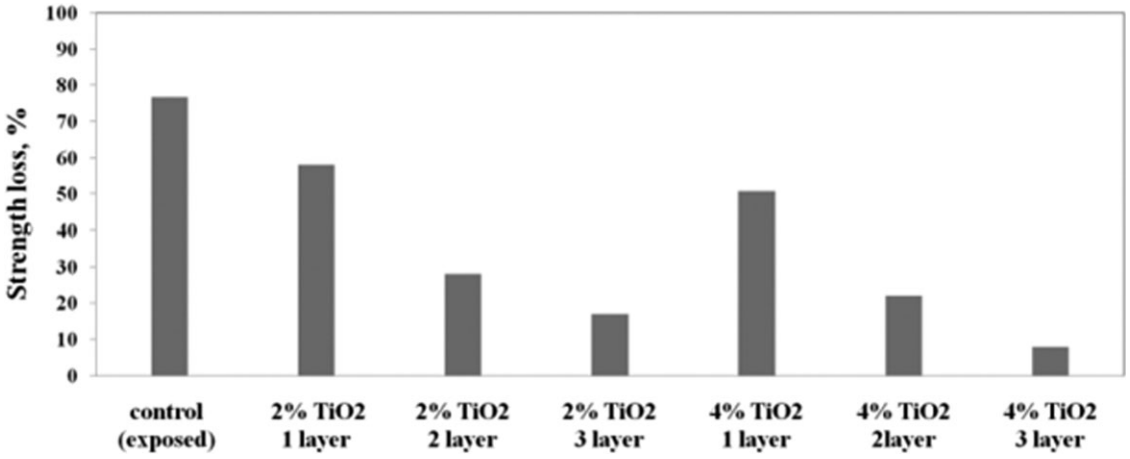

Figure 19. Tensile strength loss of the PBO yarns sheathed with PU layers containing TiO_2 after 6 days of exposure to UV–vis.

This was confirmed by the volume density results determined experimentally. The UV–vis transmittance results of the membrane prepared by the coagulation method showed that about a 45% reduction in transmittance in the visible region and more than a 50% reduction in the UV region (300–400 nm) compared to the membrane prepared by the evaporation method. This reduction in transmittance of the coagulated membrane was attributed to the opaqueness of coagulated membrane, which resulted from the irregular morphological structure, which caused more light scattering.

The effect of TiO_2 nanoparticles on the morphological structure and UV–vis light transmission of the coagulated membrane were evaluated. The SEM images of the top view and cross section of different membranes loaded with different TiO_2 nanoparticles percentages (0, 1, 2, and 4%) showed that with increasing nanoparticle percentages, the porosity of the membrane increased, and the volume density decreased. The membrane density went down from 1.05 g/cm^3 for the blank membrane to 0.552 g/cm^3 for the composite membrane loaded with 4% TiO_2 nanoparticles. The UV–vis transmittance decreased with increasing amount of TiO_2 and number of membrane layers.

The effectiveness of the composite membranes in protecting the PBO from UV–vis was evaluated. The results show that the maximum strength loss of the unprotected control PBO fiber after 6 days of exposure to UV–vis was 76.6%. The strength loss of the PBO fiber that was protected with three layers of PU loaded with 2% TiO_2 was 16.95%. The lowest strength loss of 7.8% (or maximum protection) was achieved by three layers of PU loaded with 4% TiO_2.

ACKNOWLEDGMENTS

This work was funded by NASA, Balloon Research and Development Laboratory (grant number NNXlOAE26G). The authors thank Rahul Vallabh of North Carolina State University College of Textiles for his valuable suggestions.

REFERENCES

1. Yang, H.; Zhu, S.; Pan, N. *J. Appl. Polym. Sci.* **2004**, *92*, 3201.
2. Phaneshwar, K.; Parabir, K.; Steven, B. *Polym. Degrad. Stab.* **2006**, *91*, 2437.
3. Gupta, A. M.S. Thesis, North Carolina State University, **2005**.
4. Walsh, P.; Hu, X.; Cunniff, P.; Lesser, A. *J. Appl. Polym. Sci.* **2006**, *102*, 3517.
5. Walsh, P.; Hu, X.; Cunniff, P.; Lesser, A. *J. Appl. Polym. Sci.* **2006**, *102*, 3819.
6. Xing, Y.; Ding, X. *J. Appl. Polym. Sci.* **2007**, *103*, 3113.
7. Chen, X.; Wang, Z.; Laio, Z.; Mai, Y.; Zhang, M. *Polym. Test* **2007**, *26*, 202.
8. Liu, X.; Yu, W.; Xu, P. *Fibers Polym.* **2008**, *9*, 455.
9. Said, M.; Dingwall, B.; Gupta, A.; Seyam, A.; Mock, G.; Theyson, T. *Adv. Space Res.* **2006**, *37*, 2052.
10. Hearle, J. W. High Performance Fibers; Woodhead: Cambridge, United Kingdom, **2001**.
11. Moore, R.; Weigmann, H. *Text. Res. J.* **1986**, *56*, 254.
12. Chen, L.; Young, T. J. *Membr. Sci* **1991**, *59*, 15.
13. Mulder, M. Basic Principles of Membrane Technology; Kluwer Academic: Dordrecht, The Netherlands, **1991**.
14. Salamone, J. Polymeric Materials Encyclopedia: Vol. *6*. M–O; CRC: Boca Raton, FL, **1996**.
15. Soroko, I.; Livingston, A. *J. Membr. Sci.* **2009**, *343*, 189.
16. Li, J.; Xu, Z.; Yang, H.; Yu, L.; Liu, M. *Appl. Surf. Sci.* **2009**, *255*, 4725.
17. Razmjou, A.; Mansouri, J.; Chen, V. *J. Membr. Sci.* **2011**, *378*, 73.
18. Cao, X.; Ma, J.; Shi, X.; Ren, Z. *Appl. Surf. Sci.* **2006**, *253*, 2003.